Published in final edited form as:
J Alzheimers Dis. 2011 ; 23(1): 61–77. doi:10.3233/JAD-2010-101374.

Neuroprotective and Neurorescue Effects of a Novel Polymeric Nanoparticle Formulation of Curcumin (NanoCurc™) in the Neuronal Cell Culture and Animal Model: Implications for Alzheimer's Disease

Balmiki Ray[a,1], **Savita Bisht**[b,1], **Amarnath Maitra**[d], **Anirban Maitra**[b], and **Debomoy K. Lahiri**[a,c,*]

[a]Department of Psychiatry, Institute of Psychiatric Research, Indiana University School of Medicine, Indianapolis, IN, USA

[b]The Sol Goldman Pancreatic Cancer Research Center, Department of Pathology, Johns Hopkins University School of Medicine, Baltimore, MD, USA

[c]Department of Medical and Molecular Genetics, Indiana University School of Medicine, Indianapolis, IN, USA

[d]Visvabharati University, Santiniketan, West Bengal, India

Abstract

Alzheimer's disease (AD) is characterized by deposition of amyloid-β (Aβ) plaques within the brain parenchyma followed by synaptic loss and neuronal death. Deposited Aβ reacts with activated microglia to produce reactive oxygen species (ROS) and cytochemokines, which lead to severe neuroinflammation. Curcumin is a yellow polyphenol compound found in turmeric, a widely used culinary ingredient that possesses anti-inflammatory and anti-cancer properties and may show efficacy as a potential therapeutic agent in several neuro-inflammatory diseases including AD. However, poor aqueous solubility and sub-optimal systemic absorption from the gastrointestinal tract may represent factors contributing to its failure in clinical trials. To increase curcumin's bioavailability, a polymeric nanoparticle encapsulated curcumin (NanoCurc™) was formulated which is completely water soluble. NanoCurc™ treatment protects neuronally differentiated human SK-N-SH cells from ROS (H_2O_2) mediated insults. NanoCurc™ also rescues differentiated human SK-N-SH cells, which were previously insulted with H_2O_2. *In vivo*, intraperitoneal (IP) NanoCurc™ injection at a dose of 25 mg/kg twice daily in athymic mice resulted in significant curcumin levels in the brain (0.32 μg/g). Biochemical study of NanoCurc™-treated athymic mice revealed decreased levels of H_2O_2 as well as caspase 3 and caspase 7 activities in the brain, accompanied by increased glutathione (GSH) concentrations. Increased free to oxidized glutathione (GSH : GSSH) ratio in athymic mice brain *versus* controls also indicated a favorable redox intracellular environment. Taken together, these results suggest that NanoCurc™ represents an optimized formulation worthy of assessing the therapeutic value of curcumin in AD.

*Correspondence to: Indiana University School of Medicine, 791 Union Drive, Indianapolis, IN 46202, USA. Tel.: +1 317 274 2706; Fax: +1 317 274 1365; dlahiri@iupui.edu. .

[1]B. Ray and S. Bisht have contributed equally to this manuscript.

Authors' disclosures available online (http://www.j-alz.com/disclosures/view.php?id=609).

Keywords

Alzheimer's disease; caspase; curcumin; glutathione; GSH; NanoCurc™; neuropreservation; neuroprotection; oxidative stress; polymeric nanoparticle; reactive oxygen species

INTRODUCTION

Curcumin is a yellow colored polyphenol compound obtained from the plant *Curcuma longa*. Curcumin is one of the ingredients of turmeric, which is used as a culinary compound in wide regions of Indian sub-continent and South East Asia. Due to its ability of inhibiting several pro-inflammatory transcription factors like nuclear factor kappa beta (NFκB), activated protein-1 (AP-1), peroxisome proliferator-activated receptor-γ (PPAR-γ) and signal transducer and activator of transcription-1 (STAT-1), curcumin exerts potent anticancer and anti-inflammatory activities [1, 2]. In the last decade, a growing body of experimental evidence suggests that curcumin can be used as a potential drug in the treatment of Alzheimer's disease (AD) because of its novel property of disaggregating amyloid-β (Aβ) plaques [3–5]. Deposition of Aβ mediated plaques and subsequent neuroinflammation are one of the major hallmarks of AD [6]. Generated Aβ plaques interact with microglia to produce reactive oxygen species (ROS), as well as other cytokines and chemokines causing neuronal damage [7]. A previous study has shown that Aβ peptide and generated ROS synergistically increase neuronal damage [8]. Thus, the potent anti-inflammatory properties of curcumin have identified it a promising agent in ameliorating neuroinflammation associated with AD.

Several authors have demonstrated the ability of curcumin in scavenging or neutralizing ROS in cell culture and animal models. However, one of the hindrances of curcumin as a potential therapeutic agent in the treatment of AD is its poor aqueous solubility [9], which is one reason for its low bioavailability following delivery through oral or parenteral route [10]. Furthermore, curcumin degrades in acidic, basic, and oxidative conditions, which further impairs its bioavailability [11]. Therefore, poor bioavailability of curcumin through oral administration is one of the causes of its failure to exert any significant effect in some randomized control trials for AD. In one clinical trial, following oral administration of 4 gm of curcumin daily, it was observed that the entire plasma curcumin remains as glucuronide conjugates, and that there was no significant change was observed in the plasma $A\beta_{1\text{-}40}$ levels between curcumin-treated groups and placebo [12]. However, lack of cognitive decline in the placebo group was also observed in that study. In another clinical trial, no serum curcumin was detected following oral doses of 500, 1000, 2000, 4000, 6000, and 8000 mg of curcumin [13]. It was also shown that curcumin is rapidly reduced by hepatic and gut microsomal enzymes resulting in low bioavailability [14, 15].

To increase the systemic bioavailability of curcumin, a polymeric nanoparticle encapsulated curcumin (NanoCurc™) formulation was developed, which exhibits complete solubility in aqueous media, and is readily amenable to parenteral administration [16, 17]. The aim of our study was to evaluate the effects of NanoCurc™ in protecting and preserving neuronal cells from ROS mediated damage both in cell culture and in animal models. Our results indicate that NanoCurc™ protects neuronally differentiated human neuroblastoma (SK-N-SH) cells from ROS (H_2O_2) mediated insults in a dose-dependent manner, when the cells were treated simultaneously with escalating doses of NanoCurc™ and 100 μM of ROS. Furthermore, NanoCurc™ protects and preserved neuronal phenotype, which was revealed by increased levels of neuron specific enolase (NSE) in NanoCurc™ treatment groups of differentiated human SK-N-SH cells when the cells were pre-treated with 100 μM of ROS for 24 h and post-treated with NanoCurc™ and 100 μM ROS for another 24 h. These results from cell

culture studies on neuroprotection were further validated *in vivo* using parenterally administered NanoCurc™ in cohorts of athymic mice.

H_2O_2 production in neurons *in vivo* occurs due to multiple mechanisms. For example, mitochondrial inner membrane depolarization takes place following calcium influx into the neurons which leads to formation of superoxide (O_2^-) free radicals [18]. These O_2^- free radicals are then converted to H_2O_2 by the enzymatic action of manganese (Mn)-superoxide dismutase (Mn-SOD) [19]. H_2O_2 can also be produced in the brain by several other mechanisms, including the enzymatic actions of monoamine oxidase (MAO), aldehyde oxidase, xanthine oxidase (XO), and copper (Cu)-SOD and zinc (Zn)-SOD [19, 20]. A reduction in the levels of total H_2O_2 was observed in the brain tissues of NanoCurc™-treated athymic mice *versus* mice receiving blank polymer only ("controls"). Free glutathione (GSH), which is a low molecular weight thiol compound found in all plants and animals, plays an important role in neutralizing free radicals [21]. Upon neutralizing free radicals, glutathione becomes oxidized and forms glutathione disulphide (GSSH). GSH and GSSH are collectively termed as 'total glutathione' [22].

It is noteworthy that human brain only consists of 2% of the total body weight, but consumes approximately 20% of total oxygen, which indicates that free radical generation in the brain is greater than the other organs of the body [23]. The ratio of free (GSH) to oxidized glutathione (GSSH) indicates a steady state redox potential of the cell, and is an important parameter to asses cellular stability against oxidative damage [24]. We observed increased levels of both free GSH and total glutathione (GSH + GSSH) in the brain of NanoCurc™-treated athymic mice *versus* controls. Importantly, we also observed a significant increase in the ratio of GSH to GSSH in the brain of NanoCurc™-treated mice, indicating an efficient cellular redox environment.

It was previously observed that high doses of ROS cause cellular death by inducing apoptosis [25]. We observed a decrease in the levels of pro-apoptotic enzymes caspase 3 and caspase 7 in the brain extract of NanoCurc™ treated athymic mice *versus* controls. Taken together, our results suggest that NanoCurc™ treatment prevents neuronal cells from oxidative stress caused by H_2O_2 in both cell culture and *in vivo*, and that putative mechanisms for the observed neuroprotection might stem from increased cellular free GSH levels and reduced caspase-induced apoptosis. The availability of a polymeric nanoparticle formulation of curcumin amenable to systemic delivery that crossed the blood-brain-barrier leads to free curcumin levels in the brain of the mice in this study was significantly greater than the brain levels of curcumin injected *in vivo* in an oil-based medium by another group of researchers [26]. This robust increase in the brain levels of curcumin using nanoparticle formulation is one of the prime aspects of this study, and provides a tractable strategy to harness the properties of this powerful, yet previously underutilized, antioxidant compound.

MATERIALS AND METHODS

Formulation of NanoCurc™

Materials—Ultra-pure curcumin (>99% diferuloylmethane) was purchased from Sabinsa Corporation (Piscataway, NJ, USA). Monomers such as N-isopropylacrylamide (NIPAAM), vinylpyrrolidone (VP), and acrylic acid (AA) required for polymer nanoparticle synthesis were obtained from Sigma Aldrich (St. Louis, MO, USA). NIPAAM was recrystallized with hexane; VP and AA were freshly distilled before use. Reagents for the polymerization step, including NN' methylene-bisacrylamide (MBA), ammonium persulfate (APS), and ferrous sulfate ($FeSO_4$) were also procured from Sigma and were used without further purification.

Synthesis of NanoCurc™

Polymer nanoparticles comprised of NIPAAM, VP, and AA were synthesized via free radical mechanism, according to the detailed synthesis method described previously [16, 27]. The pre-distilled monomers of NIPAAM, VP, and AA are mixed together in a molar ratio of 60 : 20 : 20, respectively, wherein NN' methylene-bis-acrylamide was used as a crosslinker. Polymerization was performed for 24 h at 30°C under an inert (nitrogen) atmosphere, using APS and $FeSO_4$ as initiator and activator, respectively. After complete polymerization, the total aqueous solution of polymer was purified using dialysis, and then lyophilized for post loading of curcumin, as previously described [16]. Typically, a 10 ml stock solution of polymeric nanoparticles (100 mg) was slowly mixed with 150 μl of curcumin solution in chloroform (10 mg/ml), and gently stirred for 15–20 min on low heating, in order to load curcumin and evaporate chloroform simultaneously. The resulting solution, corresponding to 1.5% (w/w) loading of curcumin in nanoparticles, was then snap frozen on a dry ice/acetone bath, and lyophilized to dry powder for further use.

Cell culture

Human SK-N-SH cells were obtained from American Type Culture Collection (ATCC) and stored in aliquots at −150°C. Cells were taken out from the freezer and plated in a 100 mm cell culture plate (Corning Inc., NY, USA) in the presence of Minimum Essential Medium (MEM, Sigma) supplemented with 10% FBS and 1× antibiotics (regular MEM). When the cells become 75% confluent, the existing media were replaced by regular MEM containing 10 μM all trans retinoic acid (ATRA, Sigma) to achieve neuronal differentiation as described before [28]. Cells were treated with ATRA for 13 days and then cells were taken out from the 100 mm plate by the adding trypsin EDTA (Mediatech Inc, VA, USA). Trypsinized cells were collected in a 15 ml polyethylene tube (PET) and centrifuged at 3000 × *g* for 5 min followed by aspiration of trypsin EDTA. Two ml of ATRA containing regular MEM was immediately added to the PET, and the cells were homogeneously mixed in the medium by a fire polished Pasteur pipette. Cells were counted in improved Neubauer hemocytometer by Trypan blue exclusion method as previously described [29]. After counting, 50,000 and 100,000 cells were transferred to each well of a 48-well and 24-well cell culture plates containing 250 μl and 500 μl of regular MEM respectively (Corning Inc.). Supplemented with 10 μM ATRA. Cells were allowed to settle down, and drugs were added after two day, i.e., at day 15 of differentiation.

Drug treatment

To evaluate the effect of NanoCurc™ on neuronal cell viability and toxicity, escalating doses of the drug (1 nM, 10 nM, 50 nM, 100 nM, 500 nM, 1 μM, and 5 μM) were directly dissolved in the ATRA containing low serum media (LSM), i.e., MEM with 1% FBS, which was completely dissolved in the medium and added to the wells ($n = 4$). An equivalent dose of void polymer also dissolved in LSM and added to four wells to evaluate whether any toxicity is caused by the void polymer itself. ATRA containing LSM without NanoCurc™ was added in four wells, and cells in these four wells served as 'vehicle' controls. The cells were treated for 24 h in a 48-well plate. At the end of the treatment, 200 μl of the conditioned medium (CM) was gently aspirated from each well, spun at 13000 × *g* for 2 min, and stored at −20°C for LDH analysis. The remaining medium was gently aspirated from each well, and the wells were rinsed once with ice-cold 1× Dulbecco's phosphate buffered saline to remove all traces of medium. Fifty microliters of M-PER buffer (Pierce, IL, USA) mixed with protease inhibitor cocktail (Roche mini, Roche, Indianapolis, USA) was added to each well of the plate, and the plate was shaken in a shaker for 10 min for complete lysis of the cells.

Determination of cellular viability by Cell Titer Glo® (CTG) assay

Equal volume (30 μl) of the cell lysate (CL) samples were taken into each well of a white 96-well plate (Corning), and 30 μl of Cell Titer Glo reagent (CTG, Promaga) was added to each well. CTG measures mitochondrial ATP concentration in the CL, and corresponds to the cell number in the lysate [30]. CTG assay was performed in 'Varitas' microplate luminometer (Turner Biosystems, Sunnyvale, CA, USA).

Determination of cellular toxicity by lactate dehydrogenase (LDH) assay

Cellular death due to toxicity is manifested by elevation of lactate dehydrogenase (LDH) in the medium. Equal volume of CM samples were used to determine cellular membrane damage and toxicity caused by any dose of NanoCurc™ by LDH assay as mentioned previously [1]. To determine the exact amount of LDH present in the CM, a standard curve with known amounts of rabbit muscle LDH was also performed (not shown).

Co-treatment of differentiated SK-N-SH cells with NanoCurc™ and reactive oxygen species (ROS)

Wells of a 48-well culture plate containing differentiated SK-N-SH cells were treated with five different doses of NanoCurc™ (250 nM, 500 nM, 1 μM, 2.5 μM, and 5 μM). Cells in six wells did not have any drug and served as 'vehicle'. All the cells treated with different doses of NanoCurc™ including vehicle were further co-treated with 100 μM of H_2O_2 at the same time. Treatment was carried out for 24 h. At the end of the treatment period, cells from couple of wells from each treatment groups were fixed, and cellular morphology was recorded by immunocytochemistry (ICC) technique using an inverted microscope (Leica). Cells from remaining wells were harvested. CTG and LDH assays were performed in the same way as discussed above.

Pretreatment of neuronal SK-N-SH cells with ROS and subsequent treatment with NanoCurc™ and ROS

Differentiated NK-N-SH cells were pretreated with 100 μM of H_2O_2. At the end of 24 h of pretreatment, media were aspirated out off the wells and the cells were again co-treated with two freshly prepared doses (500 nM and 1 μM) of NanoCurc™ and 100 μM of H_2O_2 for 24 h. At the end of the treatment, cellular morphology by ICC, cell viability assay by CTG, and protein analyses by Western immunoblotting were performed.

Polyacrylamide gel electrophoresis (SDS-PAGE) and Western immunoblotting analyses of cell lysate of neuronal SK-N-SH cells pretreated with ROS and subsequently treated with NanoCurc™ and ROS

Equal proteins from CL samples were loaded in 10% Bis-Tris 'Criterion' gel (BioRad) and run at 180 V for 2 h. Proteins were electrophoretically transferred onto a PVDF membrane (BioRad) using cold transfer buffer (25 mM Tris-Hcl, 200 mM glycine and 20% methanol, pH 7.6) at 30 V for 5 h at 4°C. Following transfer, the membrane was blocked in 5% nonfat milk in Tris buffered saline (pH 7.4) containing 0.05% Tween-20 (TBST) for 1 h at room temperature (RT). Thereafter, the blot was probed with polyclonal anti-NSE antibody (Abcam Inc., Cambridge, MA, USA). The antibody was diluted to 1 : 500 in 5% Milk dissolved in TBST and probed overnight at 4°C with gentle rocking. After incubation with the primary antibody, the membrane was washed three times with TBST, and subsequently probed with the secondary antibody, which was HRP-conjugated donkey anti rabbit IgG (Pierce, Rockford, IL, USA) for 1 h at RT followed by three times wash with TBST. Detection of protein band signals was achieved by adding chemoluminescent buffer (GE, Buckinghamshire, UK) to the blot, which was immediately photographed using GE chemoluminescent detection film. A specific strip of the membrane was also probed with

monoclonal anti-β actin antibody (1 : 100,000 dilutions; Sigma, St. Louis, MO, USA) for normalization purpose, and β-actin band signals were obtained in the same way as mentioned above.

Visualization of cell density and morphology by ICC

Differentiated SK-N-SH cells from two wells from each treatment group of both ROS co-treatment, and ROS pretreatment and NanoCurc™ + ROS post-treatment experiments were fixed by adding 4% paraformaldehyde (Electron Microscopy Sciences, Hatfield, PA, USA) dissolved in phosphate buffer (pH 7.4). The fixed cells were then washed three times with cold PBS and permeabilized with 0.12% Triton X-100 (Sigma) for 15 min followed by three more washes with PBS. Non-specific bindings were minimized by blocking the fixed cells for 15 min with 10% normal horse serum (Sigma) dissolved in PBS, followed by incubation with the primary antibody [monoclonal α-tubulin (Sigma) diluted 1 : 50,000 in 1% horse serum]. After overnight incubation, the cells were washed and again incubated in biotinylated donkey anti-mouse secondary antibody (Jackson immunoresearch laboratories Inc., West Grove, PA, USA) at 1 : 300 dilutions for one hour. After washing with cold PBS, the cells were incubated with a mixture of fluorescein (DTAF) conjugated streptavidin (Jackson Immunoresearch Laboratories) at 1 : 300 dilutions for 1 hour. After rinsing with PBS, 250 μl of fresh PBS mixed with 5 μM of Hoechst 33342 (Sigma) stain was added to each well for nuclear staining and examined under Leica DMIL HC inverted fluorescent microscope (Leica Microsystems GmbH, Wetzler, Germany) using the following sets of filters: for FITC (excitation of 480–520 nm, band pass of 505 nm and emission of 535–585 nm) and for nuclear staining by Hoechst 33342 (excitation of 350–400 nm, band pass of 400 nm and emission of 460–510 nm). Combination of these filters minimizes the cross-talk between the signals from individual fluorochromes. Images were captures with a SPOT RT-SE digital camera (Diagnostic Instruments, Sterling Heights, MI, USA) and superimposed using the SPOT basic software (Diagnostic Instruments). The cells stained with α-tubulin exhibited green fluorescence and nuclei stained with Hoechst 33342 appeared as blue under their respective filter sets.

Effect of NanoCurc™ treatment in athymic mice

To determine *in vivo* toxicity and steady state concentrations of curcumin in the brain, 5–6 weeks old athymic CD1 athymic mice were divided into two groups and administered either NanoCurc™ (equivalent to 25 mg/kg of curcumin) (n = 12) or void polymer (n = 6) twice daily through the intraperitoneal route for four weeks. During the course of treatment, mice were monitored daily for behavioral abnormalities or any other signs of toxicity, and the body weights were measured every week. The mice were sacrificed after 16 h of the last dose of NanoCurc™. All animal (mouse) experiments described here conformed to the guidelines of the Animal Care and Use Committee of Johns Hopkins University. Mice were maintained in accordance to the guidelines of the American Association of Laboratory Animal Care.

Measurement of curcumin concentrations in the mice brain

At the end of the 4-week treatment, brain tissues were harvested and divided into two equal halves. One half of the tissue was immediately stored in pre-chilled conditioned buffer, and the other half was snap frozen to estimate tissue curcumin levels and stored at 80°C until further use. Curcumin concentrations in–brain tissue samples were measured in the Sidney Kimmel Cancer Center Analytical core facility at Johns Hopkins using liquid chromatography and tandem mass spectrometry (LC-MS/MS), as previously described [31].

Preparation of athymic mice brain lysate

After weighing, approximately 5 mg of cortical brain tissues were taken in each of a 2 ml microfuge tube. Two hundred microliters of M-PER buffer was added to each of the tubes, and the brain samples were sonicated to generate a homogeneous lysate. The lysates were centrifuged at 13000 × *g* for 15 min, and the supernatant was transferred to properly labeled individual tubes. Protein concentration of the brain lysate was determined by standard Bradford protein assay, as previously described [32]. Protein concentration of one mice brain was too low, hence excluded from the biochemical assays. The samples were stored at −80°C for other biochemical assays.

Measurement of caspase activity in athymic mice brain lysate

Luminescence based Caspase Glo® assay (Promega, Madison, WI, USA) detects caspase 3 and caspase 7 enzymes activity in the lysate. Briefly, equal volumes (30 μl) of mice brain lysates were taken in each well of a white 96-well plate (Corning), and 30 μl of Caspase Glo reagents were added to each well. The plate was incubated for 30 min at RT, and luminescent signals ware obtained using the luminometer (Perkin-Elmer). The individual signals from each brain lysates were normalized with respective protein concentration of those samples. Before measuring caspase 3 and caspase 7 activities in all the samples, signals with different volumes from a single lysate were obtained to determine the linearity of the assay, which was found to be linear in our assay condition.

Measurement of ROS content in the athymic mice brain lysate

A fluorescence based sensitive Amplex® Red (Invitrogen) H_2O_2 reagent assay was utilized in order to determine the levels of ROS in the brain lysate of controls and NanoCurc™ treated athymic mice. The chemical substance, 10-acetyl-3,7-dihydroxyphenoxazine, present in the Amplex® Red reagent along with horseradish perxidase (HRP) reacts with H_2O_2 to produce a fluorescent oxidation product ‘resorufin’ [33], and the signals were measured in a fluorometer (Tecan). This assay can detect the concentrations of H_2O_2 present in biological samples [34, 35].

Measurement of total, free, and oxidized glutathione levels in athymic mice brain lysate

Free and total glutathione levels in the brain lysate were measured by a sensitive fluorescence based DeteX® kit (Arbor Assays, Ann Arbor, MI, USA), as per the manufacturer’s instructions. A non-fluorescent molecule ThioStar® that is present in the assay reagent, covalently binds with the thiol (–SH) group of glutathione, and produces fluorescent signal which was detected in the fluorometer (Tecan). This assay measures total glutathione and free glutathione. Levels of oxidized glutathione were determined by subtracting the levels of free glutathione from the levels of total glutathione.

Statistical analyses

Experiments were done in 4–6/treatment and biochemical assays were carried out in linear range with appropriate blanks and controls. The data were analyzed by using SPSS software (v.15). Analyses were carried out with ‘one-way ANOVA’ (for three or more groups) with Bonferroni corrections or student *t*-test (for two groups). For all analyses, a *p* value of 0.05 or lower was considered significant.

RESULTS

NanoCurc™ treatment is well tolerated by differentiated SK-N-SH cells

A wide dose range (1 nM, 10 nM, 50 nM, 100 nM, 500 nM, 1 μM, and 5 μM) of NanoCurc™ treatment showed no significant change in the viability of the differentiated

SK-N-SH cells which was evident by the CTG assay (Fig. 1A). LDH assay also confirmed that all tested doses of NanoCurc™ treatment were nontoxic to the cells (up to 5 μM dose tested) (Fig. 1B).

NanoCurc™ protects neuronally differentiated SK-N-SH cells that were subjected to ROS-mediated acute insults concomitantly with the treatment

Neuroprotection property of NanoCurc™ was assessed by co-treating differentiated SK-N-SH cells with different doses (250 nM, 500 nM, 1 μM, 2.5 μM, and 5 μM) of NanoCurc™ and 100 μM of H_2O_2 for 24 h. CTG assay revealed that NanoCurc™ protected the viability of differentiated SK-N-SH cells in a dose-dependent manner (Fig. 1C). This protection was evident as the cell viability was increased by ~30% and ~50% with 250 nM and 5 μM NanoCurc™, respectively, *versus* cells treated only with 100 μM of H_2O_2. Measurement of LDH from the CM samples also showed a dose dependent decrease in the LDH release from the cells with NanoCurc™ treatment. LDH release was decreased by 50% and ~80% with 250 nM and 5 μM NanoCurc~™ respectively *versus* cells treated with 100 μMofH_2O_2 alone (Fig. 1D). Visualization of cellular density and morphology by ICC imaging also revealed that cells treated with NanoCurc™ were protected from ROS mediated insults *versus* a significant loss of cells treated with 100 μMH_2O_2 alone (Fig. 1E).

NanoCurc™ rescues neuronally differentiated SK-N-SH cells that were subjected to ROS mediated insult prior to the treatment

Co-treatment of differentiated SK-N-SH cells with NanoCurc™ and 100 μM H_2O_2, which were initially pretreated with 100 μM H_2O_2 alone for 24 h, rescued the cells from the ongoing damage caused by ROS. For example, CTG assay showed that 24 h pretreatment with 100 μM H_2O_2 decreased the cell viability by ~60% compared to cells not treated with ROS. In contrast, cell viability increased by 25% when 500 nM or 1 μM NanoCurc™ along with ~ 100 μM H_2O_2 were added to the cells after 24 h of pre-treatment with 100 μM H_2O_2 alone, which was a statistically significant increase in viability (Fig. 2A). Visualization of the cells confirmed that NanoCurc™treatment preserves neuronal cells even after they were treated with 100 μM H_2O_2 for 24 h (Fig. 2B). Western immunoblotting signals showed that levels of NSE were significantly increased in ROS pretreated followed by ROS and NanoCurc™ post-treatment groups (both 500 nM and 1 μM NanoCurc™) *versus* only ROS treated cells (Fig. 2C) indicating preservation of neuronal phenotype.

Steady state levels of curcumin in NanoCurc™ treated athymic mice brain extract

After demonstrating the neuroprotective role of free curcumin against ROS-induced damage to the neuronal cells, we address the novelty of this polymeric nanoparticle formulation to increase the bioavailability of curcumin at modest doses and the ability of the active compound to cross the blood-brain-barrier. The steady state levels of curcumin in brain tissue samples were determined after dosing athymic mice twice daily with either NanoCurc™ or void polymer at a dose of 25 mg/kg twice daily for 4 weeks. Body weights were also monitored on a weekly basis to exclude any signs of toxicity, and no changes in body weight or behavior abnormalities were observed (data not shown). The sensitive LC-MS/MS assay readily detected curcumin in brain tissues of mice that received NanoCurc™. The average curcumin concentration in brain tissues was 0.322 μg/g (Fig. 3A). Histological evaluation of other visceral organs (liver, lungs, kidneys, and pancreas) did not reveal any morphological abnormalities (data not shown). We have also determined the brain to plasma ratio for each mouse after treatment and plotted (Fig. 3B).

Parenteral NanoCurc™ decreases the activity of caspase 3 and 7 in the rodent cortex

Caspases enzymes belong to the family of cysteine proteases which cleave proteins at specific aspertyl residues. Caspases, particularly caspase 3 and caspase 7, are considered as critical mediators of apoptosis [36]. We measured the activity of caspase 3 and caspase 7 enzymes using a sensitive luminescence based assay in the cortical lysates of controls and NanoCurc™-treated athymic mice. We observed a decrease (40%) in the activity of both caspase 3 and caspase ~ 7 in the cortex of NanoCurc™-treated mice *versus* controls (p = 0.034). Analysis was performed as relative luminescent unit (RLU) adjusted with per microgram of cortical mass and plotted relative of 'control' (Fig. 4A).

Parenteral NanoCurc™ reduces hydrogen peroxide content in rodent brain

We measured the levels of H_2O_2 in the cortical lysates of NanoCurc™ treated and control athymic mice by a sensitive fluorescence based assay. A standard curve with known amount of H_2O_2 was also prepared and plotted. The assay showed a significant (p = 0.02) decrease (25%) in the levels of brain H_2O in the NanoCurc™~ 2 treated mice *versus* controls (Fig. 4B).

Parenteral NanoCurc™ increases the levels of free glutathione in the rodent cortex

Brain free glutathione content of control and NanoCurc™ treated athymic mice was measured by a fluorometric assay kit, as described in 'Materials and methods'. Known amounts of free glutathione (in μM) were used to prepare a standard curve. The result was plotted by after converting the μM value to pmole/μg of brain tissue, which showed a highly significant (p = 0.0001) increase (>100%) in the level of free glutathione in the cortex of NanoCurc™ treated athymic mice *versus* controls (Fig. 5A).

NanoCurc™ increases the levels of total glutathione and the ratio of free to oxidized glutathione in the rodent cortex

Brain total glutathione levels in the control and NanoCurc™ treated athymic mice were measured by the same assay kit used to detect the levels of free glutathione, as described in 'Materials and methods'. The assay was performed as per manufacturer's protocol, and a standard curve with known amount of total glutathione was prepared and plotted. The results demonstrated a borderline significant increase (p = 0.049) in the levels of total glutathione in the brain lysate of NanoCurc™-treated mice *versus* control (Fig. 5B). No significant difference was observed in the levels of oxidized glutathione in the brain lysate of NanoCurc™-treated and control animals (Fig. 5C). Importantly, a significant increase (~80%) was detected in the ratio of free to oxidized glutathione in the brain lysate of NanoCurc™ treated mice *versus* controls (Fig. 5D).

DISCUSSION

AD is the most common form of dementia affecting elderly people. Due to an increase in the lifespan of the global population in addition to changes in dietary habits and lifestyle, AD has become a major public health concern all over the world [37]. The World Health Organization (WHO) has predicted that approximately 20 million people will suffer from AD by the year 2020 [38]. At least 5 million people are suffering from the disease in the United States, and this number can increase up to 14 million by the year 2050 if a curative or disease preventive medication is not discovered [1]. Apart from deposition of Aβ peptides, AD is also characterized by severe neuro-inflammation caused by elevated cytokine levels and activated microglia [39]. The NADPH oxidase present in microglia is known as PHOX. PHOX stays inactive in steady state, but becomes activated in the presence of Aβ peptides and generates superoxide free radicals, which are eventually converted to H_2O_2 [39, 40].

Although H_2O_2 is not a free radical, it can potentially generate highly reactive hydroxyl (•OH) free radicals by reacting with several reduced metal ions causing extensive neuronal damage [41]. Furthermore, H_2O_2 alone can cause extensive lipid peroxidation of the cell membrane, and may result in a number of toxic metabolites like malondialdehyde, conjugated dienes, and ethane [42, 43]. Thus, a strategy to ameliorate neuronal oxidative stress, and in particular ROS within the neuronal milieu, is likely to have benefits on neuroinflammation, potentially reducing the progress of AD.

It was previously documented that high doses of free curcumin (100 μg/ml, which corresponds to approximately 270 μM, and 10 μg/ml, which corresponds to approximately 27 μM) effectively prevent H_2O_2-mediated lipid degradation and cytolysis in renal proximal tubular epithelial cells [44]. Another study has demonstrates that gentamicin induced nephro-toxicity in rats can be attenuated by high dose (200 mg/kg/day) of orally administrated curcumin [45]. The underlying mechanism of gentamicin induced renal tubular damage is thought to be due to the generation of H_2O_2 by renal cortical mitochondria [46]. In the context of AD, it was demonstrated that moderate to high doses of curcumin protects neuronal PC12 cells from Aβ-induced oxidative damage [47]. However, whether the prevention of Aβ-mediated oxidative damage by curcumin is due to Aβ fibril disaggregation or ROS scavenging has not yet been adequately addressed. Additionally, all of these studies have used very high doses of curcumin.

A previous study observed that curcumin in low dose (500 nM and 1 μM) stimulates neurogenesis both in cell culture and animal models, which has an important implication in AD [48]. This group of researchers had also noticed that at higher doses, curcumin decreases the viability of neural progenitor cells *in vitro*. In our study, we treated differentiated SK-N-SH cells with different doses (1 nM to 5 μM) of NanoCurc™. Both cell viability and LDH toxicity assay demonstrated no toxicity to the SK-N-SH cells by NanoCurc™. In this context, we previously tested a wide range of doses of *free* curcumin in differentiated SK-N-SH cells and observed some toxicity of the cells treated with free curcumin at more than 2 μM doses, which was evident by increased in the levels of released LDH and appearance of apoptotic bodies within the cells (*data not shown*). We also observed that NanoCurc™ treatment increased the viability and reduced the toxicity of neuronal cells in a dose-dependent manner, even in the presence of 100 μM dose of H_2O_2. In addition to biochemical protection, we also confirmed that the morphology of ROS-exposed cells was preserved when they were treated with 500 nM or greater dose of NanoCurc™ (Fig. 2C). Since we challenged the cells directly with H_2O_2, and not with Aβ, we cannot conclude that the neuroprotective property of NanoCurc™ functions by scavenging H_2O_2 alone at the cellular level. The effects of NanoCurc™ in disaggregating Aβ would require separate studies. Thus, the novel observations in our study is that NanoCurc™ treatment can not only protect neuronal cells being concurrently treated with ROS, but prospectively rescue cells that have been pre-treated for variable periods of time with ROS. For example, when the cells were pre-treated with 100 μMofH_2O_2 for 24 h and then co-treated with NanoCurc™ and 100 μM of H_2O_2, both 500 nM and 1 μM doses of NanoCurc™ increased the viability of cells, which was evident by cell viability assay (CTG) and cell morphology images.

Increased levels of NSE in NanoCurc™ treatment groups also indicate that NanoCurc™ treatment preserved neuronal morphology in ROS insulted cells. Our initial experiment where differentiated SK-N-SH cells were treated with a wide range of doses of NanoCurc™ without any insults to the cells did not produce any significant increase in the cell viability (Fig. 1A). In addition, we have also explored the possibility that curcumin or NanoCurc™ could affect the AβPP processing pathway. We have recently observed that they (each at 500 nM dose) independently decreased Aβ levels by modulating AβPP in rat neuronal PC12 cells (Ray and Lahiri, manuscript under preparation), which is consistent with their

neuroprotective properties reported herein. Such novel neuro-rescue property should have significant clinical implications in the treatment of AD because ROS mediated neuronal damage has been implicated as one of the major causes for progressive dementia in elderly.

As already mentioned in the 'Introduction', the systemic bioavailability of curcumin is minimal following oral administration in both human and animal models. Some investigators suspended curcumin in an oil-based medium, and administered through the parenteral route to animals. However, the measured amounts of curcumin in brain tissues varied considerably between studies. For example, IP injections of curcumin dissolved in 0.5 N NaOH at a cumulative dose of 148 μg to C57BL6/J mice resulted in detectable amounts of curcumin in the brain [49]. To increase the bioavailability of curcumin, some active metabolites were tested in cell culture as well as *in vivo* studies. Tetrahydrocurcumin (THC) is one of the active ingredients of curcumin and, unlike curcumin, is resistant to hydrolysis and stable within a wide range of pH [50]. Although THC showed better bioavailability than that of pure curcumin, reduction in Aβ plaques was not observed in AD transgenic mice treated with THC [49]. Hence, pure curcumin still remains as the most effective in amelioration in AD pathophysiology.

Previous studies revealed that co-administration with piperine may increase the bioavailability of curcumin [51]. A recent study on rats used a high amount of curcumin (500 mg/kg) co-administered orally with 20 mg/kg piperine, which measured ~5.87 μg of curcumin in the whole brain [52]. Notably, this dose was 20 times greater than the dose of NanoCurc™ used in our present study, which clearly illustrated the effectiveness of nano strategy. Another approach for effective delivery of curcumin was carried out where free curcumin, suspended in corn oil, was injected in male Mongolian gerbils intra-peritoneally at a dose of 30 mg/kg, resulting in brain concentrations of approximately 0.15 ng/mg of protein lysate after 1 h of injection. This dose gradually decreased to approximately 0.01 ng/mg of protein lysate after 24 h of injection. No significant amount of curcumin was detectable after 48 h of injection [26].

On the contrary, we injected 25 mg/kg of NanoCurc™ intraperitoneally and the brain levels of curcumin was found to be ~0.322 ng/mg of brain tissue after 16 h of injection, which is approximately 3 to 30 times more than the brain level of curcumin found in the previous study [26]. However, brain curcumin measurement in this two studies was not carried out using identical assay formats in these two studies. Use of our nanoparticle also circumvents the need for injections with a corn oil based excipient, which would be untenable in clinical settings. This difference of 3–30 fold using NanoCurc™ indicates that nanoparticle ~ based formulation is probably one of the best ways of delivering curcumin to the brain. In this context, a separate nanoparticle formulated curcumin was recently developed, and showed to inhibit cisplatin resistant ovarian cancer cells *in vitro* [53]. However, this compound has not yet been tested in animal models of AD, and our study is the first to document neuroprotective and neuropreservatory effects of curcumin both in cell culture and *in vivo* using a bona fide 'nano-formulation'.

A previous study demonstrated that Aβ-mediated death of cultured endothelial cells was due to activation of caspase 3 and caspase 8, which can be prevented by a broad spectrum caspase inhibitor [54]. Another cell culture based study showed that treatment of primary rat neuronal cells with Aβ25-35 significantly increased the activation of caspase 3 [55]. They also found that Aβ mediated activation of caspase 3 was reduced following *in vitro* exposure to curcumin. Notably, caspase 3 positive pyramidal cells are increased in AD transgenic mice (Tg2576) brain, suggesting a putative role for deregulated apoptosis in the pathogenesis of this disease [56]. However, it is unclear whether curcumin independently decreased caspase 3 activity, the decrease was due to Aβ disaggregation, or other extraneous

factors. Our results showed that caspase 3 and caspase 7 activities were significantly decreased in the cortical lysate of NanoCurc™-treated mice, which may ameliorate pathological neuronal cell death observed in AD and other neurodegenerative diseases. Therefore, our present study may be important in the context of AD.

The unique ability of NanoCurc™ to protect and rescue neuronal cells against ROS insults provides further implications for our findings. H_2O_2, which is produced in every cell, is removed by the catalytic action of glutathione peroxidase in the presence of GSH [41]. Depletion in cellular GSH levels (with corresponding reduction in free over total glutathione) is an important measure of oxidative stress, implicated in the pathogenesis of AD and other neurodegenerative disorders. A study on postmortem brain of AD patients has revealed decreased levels of GSH in some regions of the brain *versus* controls [57]. Similarly, the GSH levels were low in the red blood cells of male AD patients *versus* control patients, further underscoring an association between GSH and AD [58]. We have measured levels of GSH in the brain homogenates of mice, and observed a significant increase in the level of this key antioxidant in the NanoCurc™-treated mice brain *versus* controls, which was consistent with the observed decrease in H_2O_2 content in this cohort. We also observed a significant increase in brain level of total glutathione (GSH + GSSH) in the treated mice group, which can most likely be accounted by two fold increase in the level of GSH. Reduced glutathione (GSSH) is converted back to GSH by glutathione reductase [59]. Notably, we did not see any significant change in brain GSSH levels in the treated group. Currently, we are exploring whether these results are due to an increase in the activity of the enzyme glutathione reductase, alteration in GSH trafficking or other protective cellular mechanisms in NanoCurc™ treated mice. Furthermore, we observed a significant increase in GSH to GSSH ratio in treated group of animals indicating an efficient free radical neutralizing ability of NanoCurc™ in brain.

Taken together, these results suggest that NanoCurc™ treatment has unique capacity to protect, preserve and rescue human neuronal cells against oxidative damage. The novel nanopartcle formulation can cross the blood-brain barrier to deliver a significant amount of curcumin in the brain of tested mice. In turn, NanoCurc™ may create a protective redox intracellular environment. In conclusion, this study demonstrates the ability of NanoCurc™ in ameliorating ROS-mediated damage in both cell culture and in animal models, which can have far reaching implications in the treatment of several neurodegenerative diseases including AD.

Acknowledgments

This work was supported by grants from Alzheimer's Associations (Zenith Award); and the National Institutes of Health (AG18379 and AG18884) to DKL and also partially supported by NIH Grant U54CA151838 and a grant from the Flight Attendants Medical Research Institute (FAMRI) to A.M. We acknowledge Michelle Rudek for performing the LC-MS/MS assay measuring curcumin levels in the brain (this assay was developed using funds from the Johns Hopkins CTSA Institute for Clinical and Translational Research [UL1RR025005], and the Hopkins Cancer Center Core grant P30CA069773). We also thank John Spence, Jason Bailey, Justin Long and Cindy Morgan.

NanoCurc™ is a registered trademark of SignPath Pharmaceuticals, Inc., Quakerstown, Pennsylvania. Dr. Maitra is a member of the scientific advisory board of SignPath Pharma, Inc., and any conflicts of interest under this arrangement are handled in accordance with the Johns Hopkins University Office of Policy Coordination (OPC) guidelines. Dr. Lahiri is a member of the scientific advisory board of QR Pharma, Inc., Randon, PA, and declaring no conflict with this work.

REFERENCES

[1]. Ray B, Lahiri DK. Neuroinflammation in Alzheimer's disease: different molecular targets and potential therapeutic agents including curcumin. Curr Opin Pharmacol. 2009; 9:434–444. [PubMed: 19656726]

[2]. Goel A, Kunnumakkara AB, Aggarwal BB. Curcumin as "Curecumin": from kitchen to clinic. Biochem Pharmacol. 2008; 75:787–809. [PubMed: 17900536]

[3]. Lim GP, Chu T, Yang F, Beech W, Frautschy SA, Cole GM. The curry spice curcumin reduces oxidative damage and amyloid pathology in an Alzheimer transgenic mouse. J Neurosci. 2001; 21:8370–8377. [PubMed: 11606625]

[4]. Durairajan SS, Yuan Q, Xie L, Chan WS, Kum WF, Koo I, Liu C, Song Y, Huang JD, Klein WL, Li M. Salvianolic acid B inhibits Abeta fibril formation and disaggregates preformed fibrils and protects against Abeta-induced cytotoxicty. Neurochem Int. 2008; 52:741–750. [PubMed: 17964692]

[5]. Reinke AA, Gestwicki JE. Structure-activity relationships of amyloid beta-aggregation inhibitors based on curcumin: influence of linker length and flexibility. Chem Biol Drug Des. 2007; 70:206–215. [PubMed: 17718715]

[6]. Lahiri DK, Farlow MR, Sambamurti K, Greig NH, Giacobini E, Schneider LS. A critical analysis of new molecular targets and strategies for drug developments in Alzheimer's disease. Curr Drug Targets. 2003; 4:97–112. [PubMed: 12558063]

[7]. Coraci IS, Husemann J, Berman JW, Hulette C, Dufour JH, Campanella GK, Luster AD, Silverstein SC, El-Khoury JB. CD36, a class B scavenger receptor, is expressed on microglia in Alzheimer's disease brains and can mediate production of reactive oxygen species in response to beta-amyloid fibrils. Am J Pathol. 2002; 160:101–112. [PubMed: 11786404]

[8]. Smith MA, Perry G, Richey PL, Sayre LM, Anderson VE, Beal MF, Kowall N. Oxidative damage in Alzheimer's. Nature. 1996; 382:120–121. [PubMed: 8700201]

[9]. Tonnesen HH, Masson M, Loftsson T. Studies of curcumin and curcuminoids. XXVII. Cyclodextrin complexation: solubility, chemical and photochemical stability. Int J Pharm. 2002; 244:127–135. [PubMed: 12204572]

[10]. Sharma RA, Gescher AJ, Steward WP. Curcumin: the story so far. Eur J Cancer. 2005; 41:1955–1968. [PubMed: 16081279]

[11]. Ansari MJ, Ahmad S, Kohli K, Ali J, Khar RK. Stability-indicating HPTLC determination of curcumin in bulk drug and pharmaceutical formulations. J Pharm Biomed Anal. 2005; 39:132–138. [PubMed: 15941643]

[12]. Baum L, Lam CW, Cheung SK, Kwok T, Lui V, Tsoh J, Lam L, Leung V, Hui E, Ng C, Woo J, Chiu HF, Goggins WB, Zee BC, Cheng KF, Fong CY, Wong A, Mok H, Chow MS, Ho PC, Ip SP, Ho CS, Yu XW, Lai CY, Chan MH, Szeto S, Chan IH, Mok V. Six-month randomized, placebo-controlled, double-blind, pilot clinical trial of curcumin in patients with Alzheimer disease. J Clin Psychopharmacol. 2008; 28:110–113. [PubMed: 18204357]

[13]. Lao CD, Ruffin MTt, Normolle D, Heath DD, Murray SI, Bailey JM, Boggs ME, Crowell J, Rock CL, Brenner DE. Dose escalation of a curcuminoid formulation. BMC Complement Altern Med. 2006; 6:10. [PubMed: 16545122]

[14]. Ireson CR, Jones DJ, Orr S, Coughtrie MW, Boocock DJ, Williams ML, Farmer PB, Steward WP, Gescher AJ. Metabolism of the cancer chemopreventive agent curcumin in human and rat intestine. Cancer Epidemiol Biomarkers Prev. 2002; 11:105–111. [PubMed: 11815407]

[15]. Bisht S, Maitra A. Systemic delivery of curcumin: 21st century solutions for an ancient conundrum. Curr Drug Discov Technol. 2009; 6:192–199. [PubMed: 19496751]

[16]. Bisht S, Feldmann G, Soni S, Ravi R, Karikar C, Maitra A. Polymeric nanoparticle-encapsulated curcumin ("nanocurcumin"): a novel strategy for human cancer therapy. J Nanobiotechnology. 2007; 5:3. [PubMed: 17439648]

[17]. Bisht S, Mizuma M, Feldmann G, Ottenhof NA, Hong SM, Pramanik D, Chenna V, Karikari C, Sharma R, Goggins MG, Rudek MA, Ravi R, Maitra A. Systemic administration of polymeric nanoparticle-encapsulated curcumin (NanoCurc) blocks tumor growth and metastases in pre-

clinical models of pancreatic cancer. Mol Cancer Ther. 2010; 9:2255–2264. [PubMed: 20647339]

[18]. Cheah KS, Chance B. The oxidase systems of Ascarismuscle mitochondria. Biochim Biophys Acta. 1970; 223:55–60. [PubMed: 4320757]

[19]. Kaminsky YG, Kosenko EA. Effects of amyloid-beta peptides on hydrogen peroxide-metabolizing enzymes in rat brain *in vivo*. Free Radic Res. 2008; 42:564–573. [PubMed: 18569014]

[20]. Maragos WF, Young KL, Altman CS, Pocernich CB, Drake J, Butterfield DA, Seif I, Holschneider DP, Chen K, Shih JC. Striatal damage and oxidative stress induced by the mitochondrial toxin malonate are reduced in clorgyline-treated rats and MAO-A deficient mice. Neurochem Res. 2004; 29:741–746. [PubMed: 15098936]

[21]. Meister A, Anderson ME. Glutathione. Annu Rev Biochem. 1983; 52:711–760. [PubMed: 6137189]

[22]. Sies H. Glutathione and its role in cellular functions. Free Radic Biol Med. 1999; 27:916–921. [PubMed: 10569624]

[23]. Richter C. Reactive oxygen and DNA damage in mitochondria. Mutat Res. 1992; 275:249–255. [PubMed: 1383767]

[24]. Smith CV, Jones DP, Guenthner TM, Lash LH, Lauterburg BH. Compartmentation of glutathione: implications for the study of toxicity and disease. Toxicol Appl Pharmacol. 1996; 140:1–12. [PubMed: 8806864]

[25]. Martindale JL, Holbrook NJ. Cellular response to oxidative stress: signaling for suicide and survival. J Cell Physiol. 2002; 192:1–15. [PubMed: 12115731]

[26]. Wang Q, Sun AY, Simonyi A, Jensen MD, Shelat PB, Rottinghaus GE, MacDonald RS, Miller DK, Lubahn DE, Weisman GA, Sun GY. Neuroprotective mechanisms of curcumin against cerebral ischemia-induced neuronal apoptosis and behavioral deficits. J Neurosci Res. 2005; 82:138–148. [PubMed: 16075466]

[27]. Bisht S, Feldmann G, Koorstra JB, Mullendore M, Alvarez H, Karikari C, Rudek MA, Lee CK, Maitra A. *In vivo* characterization of a polymeric nanoparticle platform with potential oral drug delivery capabilities. Mol Cancer Ther. 2008; 7:3878–3888. [PubMed: 19074860]

[28]. Ray B, Simon JR, Lahiri DK. Determination of high-affinity choline uptake (HACU) and choline acetyltransferase (ChAT) activity in the same population of cultured cells. Brain Res. 2009; 1297:160–168. [PubMed: 19660442]

[29]. Ray B, Bailey JA, Sarkar S, Lahiri DK. Molecular and immunocytochemical characterization of primary neuronal cultures from adult rat brain: differential expression of neuronal and glial protein markers. J Neurosci Methods. 2009; 184:294–302. [PubMed: 19720084]

[30]. Ray B, Banerjee PK, Greig NH, Lahiri DK. Memantine treatment decreases levels of secreted Alzheimer's amyloid precursor protein (APP) and amyloid beta (Abeta) peptide in the human neuroblastoma cells. Neurosci Lett. 2009; 470:1–5. [PubMed: 19948208]

[31]. Ma Z, Shayeganpour A, Brocks DR, Lavasanifar A, Samuel J. High-performance liquid chromatography analysis of curcumin in rat plasma: application to pharmacokinetics of polymeric micellar formulation of curcumin. Biomed Chromatogr. 2007; 21:546–552. [PubMed: 17340565]

[32]. Alley GM, Bailey JA, Chen D, Ray B, Puli LK, Tanila H, Banerjee PK, Lahiri DK. Memantine lowers amyloid-beta peptide levels in neuronal cultures and in APP/PS1 transgenic mice. J Neurosci Res. 2009; 88:143–154. [PubMed: 19642202]

[33]. Zhou M, Diwu Z, Panchuk-Voloshina N, Haugland RP. A stable nonfluorescent derivative of resorufin for the fluorometric determination of trace hydrogen peroxide: applications in detecting the activity of phagocyte NADPH oxidase and other oxidases. Anal Biochem. 1997; 253:162–168. [PubMed: 9367498]

[34]. Votyakova TV, Reynolds IJ. DeltaPsi(m)-dependent and -independent production of reactive oxygen species by rat brain mitochondria. J Neurochem. 2001; 79:266–277. [PubMed: 11677254]

[35]. Song C, Al-Mehdi AB, Fisher AB. An immediate endothelial cell signaling response to lung ischemia. Am J Physiol Lung Cell Mol Physiol. 2001; 281:L993–L1000. [PubMed: 11557603]

[36]. Allan LA, Clarke PR. Apoptosis and autophagy: regulation of caspase-9 by phosphorylation. FEBS J. 2009; 276:6063–6073. [PubMed: 19788417]

[37]. Bandyopadhyay S, Goldstein LE, Lahiri DK, Rogers JT. Role of the APP non-amyloidogenic signaling pathway and targeting alpha-secretase as an alternative drug target for treatment of Alzheimer's disease. Curr Med Chem. 2007; 14:2848–2864. [PubMed: 18045131]

[38]. Dufouil C, Alperovitch A. Epidemiology of Alzheimer's disease. Rev Prat. 2005; 55:1869–1878. [PubMed: 16396227]

[39]. Zekry D, Epperson TK, Krause KH. A role for NOX NADPH oxidases in Alzheimer's disease and other types of dementia? IUBMB Life. 2003; 55:307–313. [PubMed: 12938732]

[40]. Jekabsone A, Mander PK, Tickler A, Sharpe M, Brown GC. Fibrillar beta-amyloid peptide Abeta1 40 activates microglial proliferation via stimulating TNF-alpha–release and H_2O_2 derived from NADPH oxidase: a cell culture study. J Neuroinflammation. 2006; 3:24. [PubMed: 16959029]

[41]. Benzi G, Moretti A. Are reactive oxygen species involved in Alzheimer's disease? Neurobiol Aging. 1995; 16:661–674. [PubMed: 8544918]

[42]. Borkan SC, Schwartz JH. Role of oxygen free radical species in *in vitro* models of proximal tubular ischemia. Am J Physiol. 1989; 257:F114–F125. [PubMed: 2750916]

[43]. Paller MS, Hebbel RP. Ethane production as a measure of lipid peroxidation after renal ischemia. Am J Physiol. 1986; 251:F839–F843. [PubMed: 3777180]

[44]. Cohly HH, Taylor A, Angel MF, Salahudeen AK. Effect of turmeric, turmerin and curcumin on H_2O_2-induced renal epithelial (LLC-PK1) cell injury. Free Radic Biol Med. 1998; 24:49–54. [PubMed: 9436613]

[45]. Farombi EO, Ekor M. Curcumin attenuates gentamicin-induced renal oxidative damage in rats. Food Chem Toxicol. 2006; 44:1443–1448. [PubMed: 16814915]

[46]. Walker PD, Shah SV. Evidence suggesting a role for hydroxyl radical in gentamicin-induced acute renal failure in rats. J Clin Invest. 1988; 81:334–341. [PubMed: 3123518]

[47]. Park SY, Kim HS, Cho EK, Kwon BY, Phark S, Hwang KW, Sul D. Curcumin protected PC12 cells against beta-amyloid-induced toxicity through the inhibition of oxidative damage and tau hyperphosphorylation. Food Chem Toxicol. 2008; 46:2881–2887. [PubMed: 18573304]

[48]. Kim SJ, Son TG, Park HR, Park M, Kim MS, Kim HS, Chung HY, Mattson MP, Lee J. Curcumin stimulates proliferation of embryonic neural progenitor cells and neurogenesis in the adult hippocampus. J Biol Chem. 2008; 283:14497–14505. [PubMed: 18362141]

[49]. Begum AN, Jones MR, Lim GP, Morihara T, Kim P, Heath DD, Rock CL, Pruitt MA, Yang F, Hudspeth B, Hu S, Faull KF, Teter B, Cole GM, Frautschy SA. Curcumin structure-function, bioavailability, and efficacy in models of neuroinflammation and Alzheimer's disease. J Pharmacol Exp Ther. 2008; 326:196–208. [PubMed: 18417733]

[50]. Pan MH, Huang TM, Lin JK. Biotransformation of curcumin through reduction and glucuronidation in mice. Drug Metab Dispos. 1999; 27:486–494. [PubMed: 10101144]

[51]. Anand P, Kunnumakkara AB, Newman RA, Aggarwal BB. Bioavailability of curcumin: problems and promises. Mol Pharm. 2007; 4:807–818. [PubMed: 17999464]

[52]. Suresh D, Srinivasan K. Tissue distribution & elimination of capsaicin, piperine & curcumin following oral intake in rats. Indian J Med Res. 2010; 131:682–691. [PubMed: 20516541]

[53]. Yallapu MM, Maher DM, Sundram V, Bell MC, Jaggi M, Chauhan SC. Curcumin induces chemo/radio-sensitization in ovarian cancer cells and curcumin nanoparticles inhibit ovarian cancer cell growth. J Ovarian Res. 2010; 3:11. [PubMed: 20429876]

[54]. Xu J, Chen S, Ku G, Ahmed SH, Chen H, Hsu CY. Amyloid beta peptide-induced cerebral endothelial cell death involves mitochondrial dysfunction and caspase activation. J Cereb Blood Flow Metab. 2001; 21:702–710. [PubMed: 11488539]

[55]. Qin XY, Cheng Y, Cui J, Zhang Y, Yu LC. Potential protection of curcumin against amyloid beta-induced toxicity on cultured rat prefrontal cortical neurons. Neurosci Lett. 2009; 463:158–161. [PubMed: 19631254]

[56]. Niu YL, Zhang WJ, Wu P, Liu B, Sun GT, Yu DM, Deng JB. Expression of the apoptosis-related proteins caspase-3 and NF-kappaB in the hippocampus of Tg2576 mice. Neurosci Bull. 2010; 26:37–46. [PubMed: 20101271]

[57]. Gu M, Owen AD, Toffa SE, Cooper JM, Dexter DT, Jenner P, Marsden CD, Schapira AH. Mitochondrial function, GSH and iron in neurodegeneration and Lewy body diseases. J Neurol Sci. 1998; 158:24–29. [PubMed: 9667773]

[58]. Liu H, Harrell LE, Shenvi S, Hagen T, Liu RM. Gender differences in glutathione metabolism in Alzheimer's disease. J Neurosci Res. 2005; 79:861–867. [PubMed: 15693022]

[59]. Joshi G, Aluise CD, Cole MP, Sultana R, Vore M, Clair DK, Butterfield DA. Alterations in brain antioxidant enzymes and redox proteomic identification of oxidized brain proteins induced by the anti-cancer drug adriamycin: implications for oxidative stress-mediated chemobrain. Neuroscience. 2010; 166:796–807. [PubMed: 20096337]

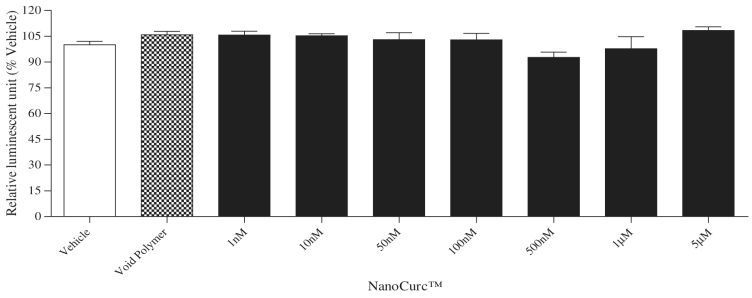

Fig. 1.

(A) Differentiated SK-N-SH cells were treated with different doses of NanoCurc™ for 24 h. After the treatment, cells were lysed using M-PER buffer, and an equal volume (30 μl) of the cell lysate from each treatment group was mixed with 30 μl of CTG assay buffer to determine the cell viability in each treatment group. Luminescence signals were obtained from the Tecan luminometer. CTG data indicate no significant increase or decrease in the viability of differentiated SK-N-SH cells following NanoCurc™ treatment.

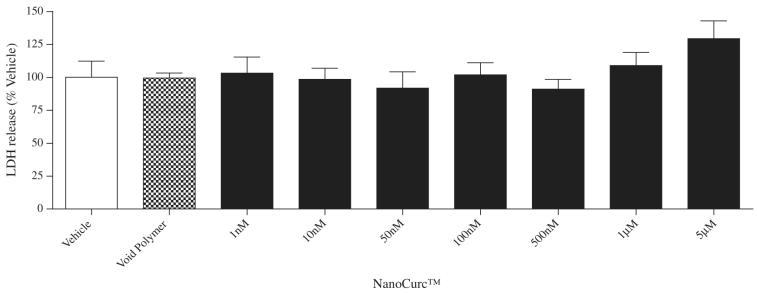

Fig. 1.

(B) Levels of LDH were measured in an equal volume (30 μl) of conditioned medium (CM) samples of each treatment group of the previous experiment to evaluate any toxicity caused by NanoCurc™ to differentiated SK-N-SH cells. LDH assay revealed that a wide range of doses of NanoCurc™ is non-toxic and well tolerated by the cells.

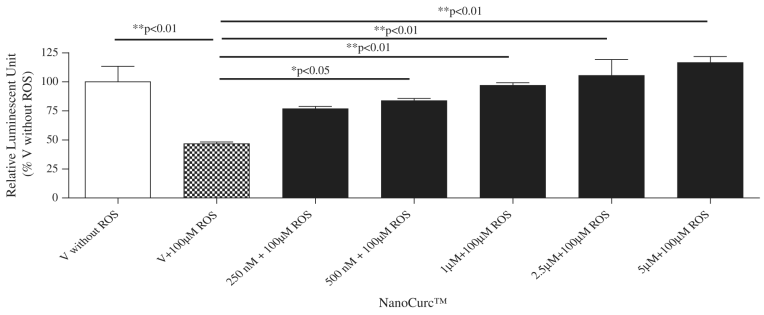

Fig. 1.

(C) Differentiated SK-N-SH cells were treated with five different doses of NanoCurc™ (250 nM, 500 nM, 1 μM, 2.5 μM, and 5 μM). Cells in four wells did not have any drug and served as 'vehicle'. All cells including the 'vehicle' were co-treated at the same time with 100 μM of H_2O_2. NanoCurc™ and H_2O_2 co-treatment was carried out for 24 h. The cells were harvested using M-PER buffer, and CTG assay was performed as described in 'Materials and methods' and in Fig. 1A. CTG result indicates that all doses of NanoCurc™ significantly protect differentiated SK-N-SH cells from H_2O_2 mediated damage.

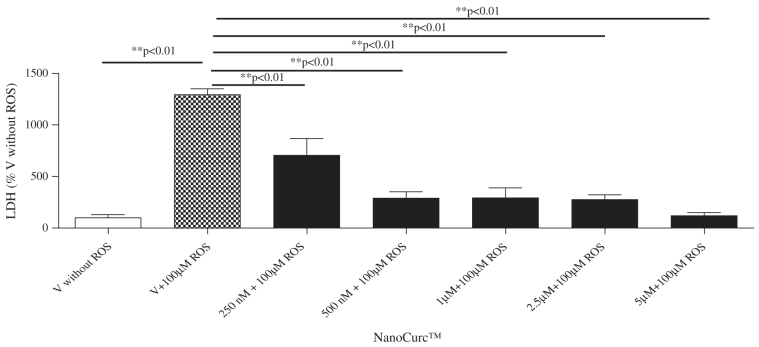

Fig. 1.

(D) Cellular toxicity (LDH) assay was performed in the same experiment with equal volumes of CM samples, which revealed that all doses of NanoCurc™ significantly decreases the toxic effects of H_2O_2 mediated insult and LDH release to the differentiated SK-N-SH cells.

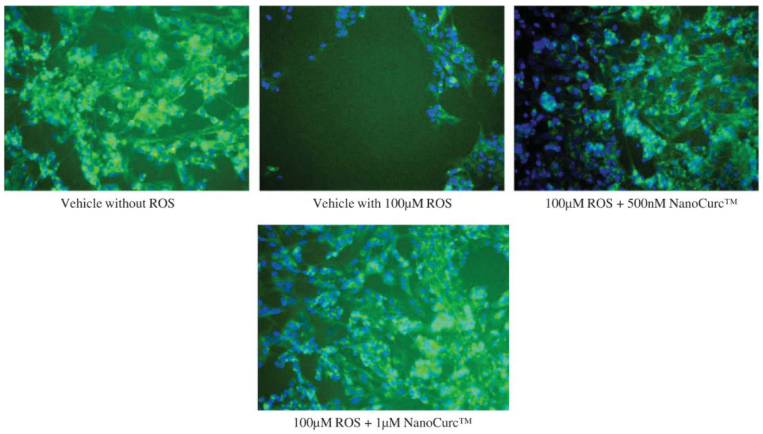

Fig. 1.

(E) Visualization of cellular density of differentiated SK-N-SH cells was carried out by ICC after 24 h of co-treatment with NanoCurc™ and 100 μM of H_2O_2. A gross decrease in the cell number was noticed in the cells which were only treated with 100 μM of H_2O_2. However neuronal cells were preserved by treatment with NanoCurc™ (Green = cytoskeletal structure stained with α tubulin; Blue = nuclear staining by Hoechst 33342).

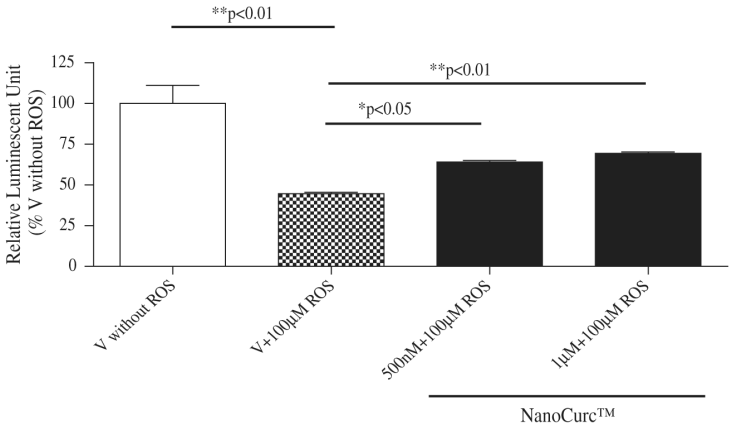

Fig. 2.

(A) Differentiated NK-N-SH cells were pretreated with 100 μM of H_2O_2 for 24 h. The media was then aspirated out off the wells, and subsequently cells were co-treated with freshly prepared two doses (500 nM and 1 μM) of NanoCurc™ and 100 μM of H_2O_2 or only vehicle + 100 μMofH_2O_2 (vehicle) for 24 h. At the end of the treatment, CTG assay was performed, which showed a significant increase in the viability of the differentiated SK-N-SH cells with both the doses of NanoCurc™ even in the presence of H_2O_2.

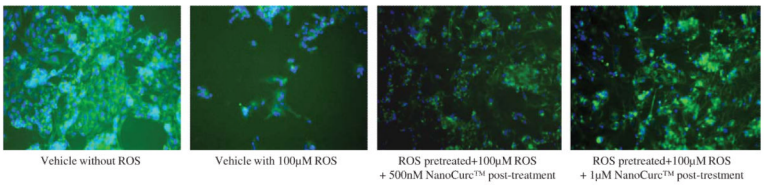

Fig. 2.

(B) Cell density observed by the ICC technique in the experiment mentioned in 'Fig. 3A' revealed that NanoCurc™ treatment preserves neuronal cells following treatment with 100 $\mu M H_2O_2$ for 24 hours and subsequent co-treatment with 100 $\mu M H_2O_2$ and two independent doses (500 nM and 1 μM) of the drug *versus* cells pre and post-treated with 100 μM of H_2O_2 only (Green = cytoskeletal structure stained with α tubulin; Blue = nuclear staining by Hoechst 33342).

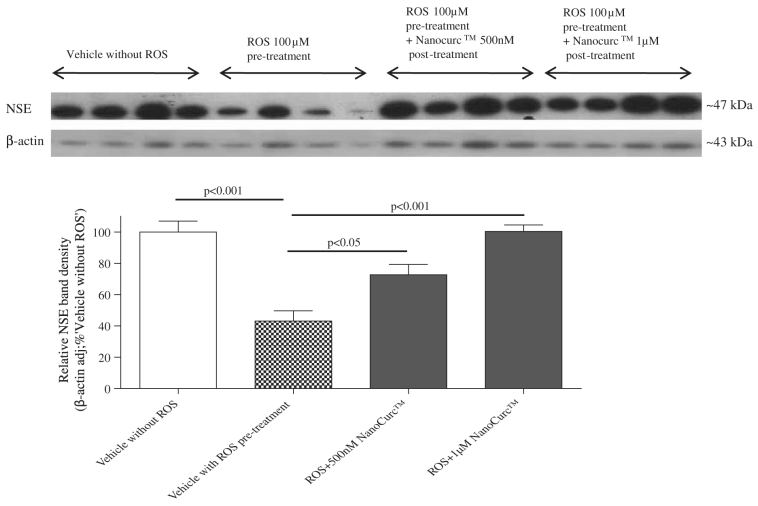

Fig. 2.

(C) Cell lysate samples from the experiment, mentioned in 'Fig. 3A' were denatured and equal amounts of protein were analyzed by SDS-PAGE. Proteins from the gel were transferred in PVDF membrane and probed with NSE and β-actin antibodies. β-actin-adjusted NSE band densities showed a significant increase in the ROS pretreated followed by ROS and NanoCurc™ treated samples compared to only the ROS treated cells.

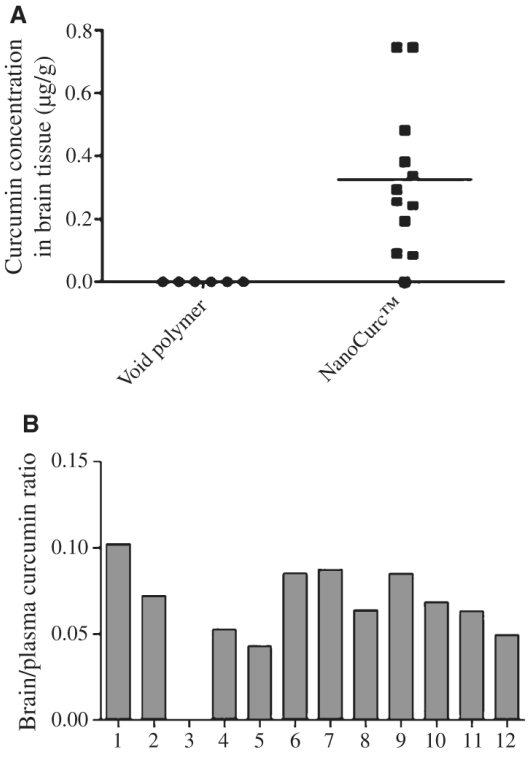

Fig. 3.

(A) The brain levels of curcumin were measured after 16 h of the last injection of NanoCurc™ using liquid chromatography and tandem mass spectrometry. Curcumin concentrations were shown as μg/g of brain tissue. Brain curcumin concentration in one mouse was below the detectable range. (B) Brain/plasma ratio: brain/plasma ratio was determined from the corresponding *in vivo* experiment where each animal (n = 12) received NanoCurc™ at a dose of 25 mg/kg BID intraperitoneally.

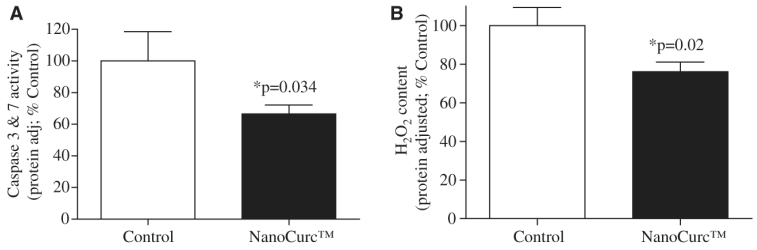

Fig. 4.

(A) A sensitive luminescence based assay was used to detect Caspase 3 and caspase 7 enzymes activity in the brain lysate of controls and NanoCurc™ treated nude mice. Individual luminescent signal from each brain lysates was normalized with respective protein concentration of the respective sample. These findings revealed a significant decrease in levels of caspase 3 and caspase 7 activities in the brain lysate of the treated group *versus* control group. (B) A sensitive fluorescence based sensitive assay was used to detect the levels of ROS (H_2O_2) in the brain lysate of controls and NanoCurc™ treated nude mice. Obtained fluorescence signal was normalized with the total protein content of the respective sample. The result showed a significant decrease in the total H_2O_2 levels in the brain lysate of the treatment group *versus* controls.

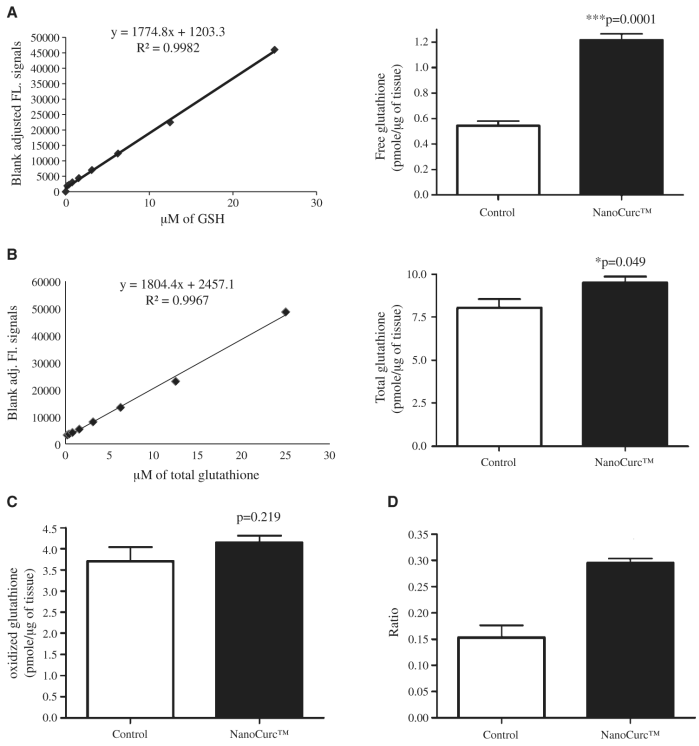

Fig. 5.

(A) A sensitive fluorescence based sensitive assay was used to assess free glutathione levels in the brain lysate of controls and NanoCurc™ treated mice. Fluorescence signals were normalized with the protein content of the brain lysate samples and plotted as pmole/µg. A significant increase in the levels of GSH was observed in the lysate of the treated mice *versus* controls. A standard curve with known amount of GSH was also shown in the left. (B) The levels of total glutathione (GSH+GSSH) was measured by the same fluorescent based assay as shown in Fig. 5A, which revealed a significant increase in the levels of total glutathione in the lysate of NanoCurc™ treated mice *versus* controls. (C) Levels of oxidized GSH were measured and no difference in the levels of oxidized GSH was observed in the lysate of NanoCurc™ treated mice *versus* controls. (D) A significant increase was observed in the ratio of GSH to GSSH in the brain lysate of NanoCurc™ treated mice *versus* controls, indicating an effective redox cellular environment by NanoCurc™ treatment to athymic mice.